frontiers | Frontiers in Marine Science

TYPE Original Research
PUBLISHED 17 February 2023
DOI 10.3389/fmars.2023.1145048

OPEN ACCESS

EDITED BY
Guang Gao,
Xiamen University, China

REVIEWED BY
Shanying Tong,
Ludong University, China
Xianghai Tang,
Ocean University of China, China
Feng Liu,
Institute of Oceanology (CAS), China

*CORRESPONDENCE
Wei Zhou
wzhou@jou.edu.cn
Juntian Xu
jtxu@jou.edu.cn

†These authors have contributed equally to this work

SPECIALTY SECTION
This article was submitted to Marine Ecosystem Ecology, a section of the journal Frontiers in Marine Science

RECEIVED 15 January 2023
ACCEPTED 09 February 2023
PUBLISHED 17 February 2023

CITATION
Cai J, Ni J, Chen Z, Wu S, Wu R, He C, Wang J, Liu Y, Zhou W and Xu J (2023) Effects of ocean acidification and eutrophication on the growth and photosynthetic performances of a green tide alga *Ulva prolifera*. *Front. Mar. Sci.* 10:1145048. doi: 10.3389/fmars.2023.1145048

Effects of ocean acidification and eutrophication on the growth and photosynthetic performances of a green tide alga *Ulva prolifera*

Jianping Cai[1,2,3], Jiaxuan Ni[1,2,3], Zeyu Chen[1,2,3], Shiqi Wu[1,2,3], Ruijie Wu[1,2,3], Chuang He[1,2,3], Jinguo Wang[1,2,3], Yili Liu[1,2,3], Wei Zhou[1,2,3*†] and Juntian Xu[1,2,3*†]

[1]Key Laboratory of Coastal Salt Marsh Ecosystems and Resources Ministry of Natural Resources, Jiangsu Ocean University, Lianyungang, China, [2]Jiangsu Key Laboratory of Marine Bioresources and Environment, Jiangsu Ocean University, Lianyungang, China, [3]Co-Innovation Center of Jiangsu Marine Bio-Industry Technology, Jiangsu Ocean University, Lianyungang, China

With the impact of fossil fuel burning and industrialization, atmospheric CO_2 concentration will reach about 1000 ppmv in 2100, and more and more CO_2 will be absorbed by ocean, resulting in ocean acidification. The Chinese coastal waters are showing unexpectedly high levels of acidification due to a combination of global ocean acidification and severe regional eutrophication, which is caused by natural accumulation or human activities such as aquacultural tail water input, potentially affecting macroalgal blooms. However, little is known about the combined effects of ocean acidification and entrophication on the eco-physiology of bloom-forming macroalgae. This study investigated *Ulva prolifera*, a dominant species causing green tide in the South Yellow Sea, and explored its growth and physiological responses under the combination conditions of ocean acidification and enriched nutrients. In this study, *U. prolifera* thalli were cultured under two CO_2 conditions (air and 1000 μatm) and two nutrient conditions (High Nutrient, HN, 135 μmol L^{-1} N and 8.5 μmol L^{-1} P; Normal Nutrient, NN, 27 μmol L^{-1} N and 1.7 μmol L^{-1} P). The results showed that eutrophication conditions obviously enhanced the relative growth rate and photosynthetic performance of *U. prolifera*. Elevated pCO_2 had no significant effect on *U. prolifera* growth and photosynthetic performance under normal nutrient conditions. However, under eutrophication conditions elevated pCO_2 inhibited *U. prolifera* growth. Moreover, eutrophication conditions markedly improved the contents of chlorophyll *a*, chlorophyll *b* and nitrate reductase activity and inhibited the soluble carbohydrate content, but elevated pCO_2 had no significant effect on them under nutrient-replete conditions. In addition, elevated pCO_2 significantly reduced the carotenoid content under eutrophication conditions and had no effect on it under normal nutrient conditions. These findings indicate that seawater eutrophication would greatly accelerate *U. prolifera* bloom, which may also be suppressed to a certain extent

by ocean acidification in the future. The study can provide valuable information for predicting the future outbreaks of *U. prolifera* green tide in nearshore regions.

KEYWORDS

ocean acidification, eutrophication, *Ulva prolifera*, green tide, growth, photosynthetic performance

1 Introduction

Green tides are mainly caused by excessive algal growth and blooms of *Ulva* spp. in a suitable natural environment, which can lead to environmental degradation and have a negative ecological impact (Wu et al., 2018). *Ulva* spp. have thin sheet-like thallus with two cell layers and a large surface area to volume ratio, which provide an easier ability to obtain nutrients and light (Reidenbach, 2017). As a group of opportunistic macroalgae, *Ulva* spp. have a wide range of environmental tolerances and are able to grow and reproduce rapidly in nutrient-rich waters (Tan et al., 1999). They had 594 species listed on AlgaeBase and could be found worldwide including coastal aquaculture, fishing, and coastal tourism and other ecological services.

The geographical distribution of green tide caused by *Ulva* spp. is mainly in the north temperate zone and involves more than 37 countries and 114 regions, such as the United States, Europe and Asia (Ye et al., 2011; Kang et al., 2021). When the green tide breaks, thalli decompose into the water column and change the chemical characteristics and biological community structure, which impacts the cultural landscape and mariculture (Franz and Friedman, 2002). In Asia, Japan firstly reported the green tide caused by *Ulva* spp. in 1995, and the green tide area reached 27.1 hectares in 2002 (Yabe et al., 2009). The green tide in the Yellow Sea of China was firstly reported in 2007, and in 2010 the green tide covered an area of 400 km^2 (Zhang et al., 2013). In 2016, the total biomass of green tide was as high as 1.17 million tons (Xiao et al., 2019). Some studies have reported that the seaweed cultivation area in the northern Jiangsu shoal had a significant contribution to the original biomass accumulation of floating *U. prolifera*. When the culture raft frame and cables were cleaned, about 62.3% of the green algae biomass would float on the sea surface and become the initial green tide floating plaque (Wang et al., 2015).

Based on classical morphological methods and molecular techniques, it is concluded that *U. prolifera is* the main dominant species causing green tide in the Yellow Sea. It has a complex life history and a variety of reproduction modes, which is the important reason for becoming the dominant species of green tide in the Yellow Sea (Cui et al., 2018; Huo et al., 2021). In addition, natural environment changes, such as global warming, greenhouse effect and nearshore eutrophication, are also potentially important driving factors for green tide outbreaks since 2007 in China (Xu et al., 2017).

Carbon dioxide concentration in the atmosphere, which increased by more than 40% since the beginning of Industrial Revolution in the 1760s, reached 415 µatm in 2021 and will reach nearly 1000 µatm by the end of this century (Hoegh-Guldberg et al., 2007; Feely et al., 2009; Gattuso et al., 2015). Nearly one-third of the anthropogenic CO_2 in the atmosphere has been absorbed in the surface waters of ocean, resulting in a decrease in surface seawater pH, a process known as ocean acidification. (Hoegh-Guldberg et al., 2007; Doney et al., 2009).

Studies have shown that elevated pCO_2 increased the growth rates of *U. fasciata* (Barakat et al., 2021) and *U. lactuca* (Olischläger et al., 2013). However, elevated pCO_2 had no significant effect on the growth of *U. linza* under nutrient-rich conditions, at elevated pCO_2, higher temperature reduced the growth of *U. linza* (Gao et al., 2018; Gao et al., 2019a). The above studies showed that the effects of elevated pCO_2 on *Ulva* spp. might be species-specific. Moreover, elevated pCO_2 increased the photosynthetic quantum yield of *U. prolifera* under low light levels but induced higher non-photochemical quenching (NPQ) under high light levels (Liu et al., 2012). Ocean acidification also affected the photosynthetic pigment contents of *Ulva* spp. The chlorophyll *a* and chlorophyll *b* synthesis of *U. lactuca* and *U. linza* were inhibited under high CO_2 level and long photoperiods (Olischläger et al., 2013; Yue et al., 2019), and the carotenoid content of *U. prolifera* was significantly reduced under a high CO_2 level (Sun et al., 2021).

The *Ulva* spp. undergoes a physiological transition from almost exclusive bicarbonate utilization to predominant carbon dioxide utilization under high CO_2 concentration conditions (Young and Gobler, 2016; Reidenbach, 2017). It has been reported that the growth rates of *Ulva* spp. were significantly increased by the interaction of ocean acidification and eutrophication. High CO_2 level significantly increased the growth rates of *Ulva* spp. and promoted the accumulation of algal biomass under eutrophication conditions. However, these studies of elevated-CO_2 were conducted indoors, without consideration of natural light and the interactive influence of CO_2 and other environmental factors (Cruces et al., 2019). The nearshore eutrophication of Jiangsu Province in China may be related to the input of a large amount of fermented chicken manure (FCM) since 2005. It was estimated that at least 50,000 tons of FCM were used for rotifer culture in ponds every year. Mariculture tail water discharged to the nearshore waters through canals, resulting in eutrophication (Liu et al., 2013). Until now, research regarding the effect of ocean acidification on harmful macroalgae has focused on laboratory studies or single-factor experiments. Relatively little is known about how *U. prolifera* grown under nearshore eutrophication conditions respond to ocean acidification.

Therefore, here we actually simulated the nearshore eutrophication and ocean acidification outside to study the synergistic effects of global climate change and seawater eutrophication on *U. prolifera*, which will provide important theoretical guidance for understanding the coping strategies of *U. prolifera* green tides in the future.

2 Materials and methods

2.1 Sample collection and culture conditions

U. prolifera was collected from the offshore area of Qingdao, Shandong Province (119°54′00″ E, 35°42′00″ N), in April 2022. The thalli were brought back to the laboratory in an incubator (4-6°C) with some ice packs and washed with filtered natural seawater to remove contaminants on the surface. The schematic diagram of the experimental design was shown in Figure 1. The algae were cultured under two nutrient levels (High Nutrient, HN: 135 μmol L^{-1} N and 8.5 μmol L^{-1} P; Normal Nutrient, NN: natural seawater collected from 24 nautical miles offshore, 27 μmol L^{-1} N and 1.7 μmol L^{-1} P) and two CO_2 conditions (HC:1000 μatm; LC: air, 425 μatm). Adding N ($NaNO_3$) and P (NaH_2PO_4) to natural seawater to make a HN medium (135 μmolL^{-1} N and 8.5 μmol L^{-1} P). LC was maintained by bubbled with ambient air, and HC was achieved from a CO_2 enricher. The experiment materials were cultured in the flasks (500 mL), and then carried out outdoor in the 500 L stainless steel water tank. The incubation temperature was controlled at 20°C (± 0.5°C) by using a chiller. The initial weight of algae was 0.05 g in each treatment group and three parallels were set for each treatment group. The seawater medium was changed every two days. The total alkalinity (TA) was measured by the method of hydrochloric acid titration and the pH value was measured using a pH meter (Zhou et al., 2022). The other chemical parameters of the carbonate system were calculated by the CO2SYS software according to the TA and pH values (Lewis et al., 1998).

2.2 Measurement of environment solar radiation

The real-time solar radiation in the natural environment was regularly monitored and recorded every minute through an outdoor solar radiation receiver (ML-020P, EKO, Japan).

2.3 Measurement of growth

The algae were taking out from the culture bottles and the water on the surface was removed using dry paper towels, the fresh algae were then weighed with an electronic balance every two days, the relative growth rate (RGR) was calculated by the following formula (Wu et al., 2010):

$$RGR(\%\, day^{-1}) = ln(W_t/W_0)/t \times 100. \quad (1)$$

where t represents the number of culture days; W_t represents the fresh weight of the algae after culturing for t days; W_0 represents the fresh weight of the algae at the beginning.

After measurement, the fresh weight of algae restored to the initial weight (0.05g) and placed in a culture flask to continue culturing.

2.4 Measurement of chlorophyll fluorescence

Chlorophyll fluorescence parameters were determined using a handheld chlorophyll fluorometer PAM (Aquapen AP 100, Czech Republic). Effective quantum yield (Yield) was recorded every 2 h from 8:00 am to 6:00 pm. Actinic light was set with 8 different light

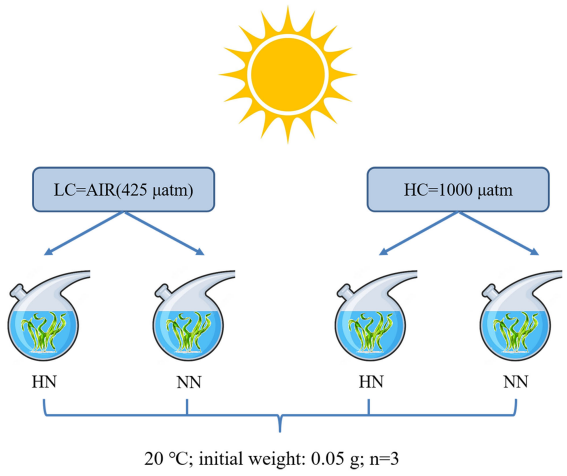

FIGURE 1
The schematic diagram of the experimental design. HN=135 μmol L^{-1} N, 8.5 μmol L^{-1} P; NN=27 μmol L^{-1} N, 1.7 μmol L^{-1} P.

intensity gradients (0, 10, 20, 50, 100, 200, 500 and 1000 μmol photons m^{-2} s^{-1}). The saturation pulse was set to 5000 μmol photons $m^{-2}s^{-1}$ (0.8 s). Relative electron transfer rate (rETR) was calculated by the following formula (Genty et al., 1989):

$$rETR(\mu mol \quad photons \quad m^{-2} \quad s^{-1}) = Yield \times 0.5 \times PAR \qquad (2)$$

where *Yield* is the photosynthetic effective quantum yield; 0.5 represents the ratio of absorbed light energy to total incident light energy; PAR is the actinic optical density (μmol photons m^{-2} s^{-1}).

2.5 Measurement of photosynthetic rate

Net photosynthetic oxygen evolution of the algae was measured using a Clark-type oxygen electrode (YSI Model 5300A, USA). The algae were cut into segments scissors of about 1 cm length and then placed under culture conditions for more than 2 h to minimize mechanical damage. The measurement temperature was maintained at 20°C using circulating water system, which was consistent with the growth temperature. About 0.04 g segments were transferred to a reaction chamber with 8 ml of culture seawater medium. 8 PAR levels (0, 10, 20, 50, 100, 200, 500 and 1000 μmol photons m^{-2} s^{-1}) were selected to measure the photosynthetic oxygen evolution rate of the algae. Data were measured and recorded every 30 s at each PAR level to analyze and obtain the P-I curve of algae photosynthesis (Henley, 1993; Ralph and Gademann, 2005).

2.6 Measurement of photosynthetic pigments

About 0.04 g of fresh thalli were soaked in 5 ml methanol at 4° C for 24 h in darkness. The absorbance values at the wavelengths of 666 nm, 665 nm, 653 nm, 652 nm and 470 nm were measured by a ultraviolet spectrophotometer. The formulas for calculating the contents of chlorophyll *a* (Chl *a*), chlorophyll *b* (Chl *b*) and carotenoids (Car) were calculated according to Wellburns's method (Wellburn, 1994; Kühl et al., 2005).

2.7 Measurement of soluble carbohydrates

The content of soluble carbohydrates was determined by an anthrone sulfate colorimetric method (Deriaz, 1961). Approximately 0.01 g of fresh thalli were ground in a mortar with a 5 ml extraction solution (0.1 mol L^{-1} phosphate buffer, pH 6.8). Grinding thalli were transferred to a boiling water bath for 1 h and then centrifuged for 10 min at 5000 g. Approximately 1 ml supernatant mixed with 4 ml 0.2% anthrone sulfate solution was continued to boil in a water bath for 10 min and then cooled down to room temperature. The absorbance value at 620 nm was determined to calculate the soluble carbohydrate (SC) content of the algae.

2.8 Measurement of soluble protein

Approximately 0.01 g of fresh thalli were ground in a mortar with 5 ml extraction solution (0.1 mol L^{-1} phosphate buffer, pH 6.8). Grinding thalli were transfer to an ice bath and then centrifuged at 5000 g for 10 min at 4°C. According to Bradford assay (Bradford, 1976), 1 ml supernatant mixed with 5 ml Coomassie brilliant blue staining solution were used to measure the absorbance value at 595 nm. The content of soluble protein (SP) was calculated with bovine serum albumin as the standard.

2.9 Assessment of nitrate reductase activity

Nitrate reductase activity (NRA) of thalli was measured using a nitrate reductase (NR) activity detection kit (Sangon Biotech D799303-0050). Approximately 0.05 g of fresh thalli was ground to obtain the nitrate reductase extract that mixed with the reaction solution to measure the initial absorbance value A_1 of the sample at 340 nm and then measure the absorbance value A_2 at 340 nm after 30 mins at 25°C. The nitrate reductase (NR) activity was calculated according to the following formula:

$$NR(U/g) = 5.359 \times \delta A/W\,. \qquad (3)$$

Where δA is the difference between the change of the absorbance value of the sample and the change of the blank absorbance; W is the fresh weight of the algae.

2.10 Data analysis

Origin 2019 and SPSS 24.0 softwares were used for statistical analysis and chart drawing of the data in this experiment, and the results were expressed as the means ± standard deviation of three replicates. The experimental data conformed to a standard normal distribution ($P > 0.05$), and homogeneity of variance was considered equal ($P > 0.05$). Two-way analysis of variance (ANOVA) was used to analyze the interactive effects of pCO_2 and nutrient concentrations on relative growth rate, carbonate system parameters, photosynthetic rate, chlorophyll fluorescence parameters, chlorophyll *a*, chlorophyll *b*, carotenoids, nitrate reductase activity, soluble protein and soluble carbohydrates. One-way analysis of variance was applied when the data complied with homogeneity of variance. Tukey's honest significant difference was applied to compare the mean values between treatments groups. The significance level was set as $P< 0.05$.

3 Results

3.1 Ambient solar radiation

The variability of ambient solar radiation during the experiment was shown in Figure 2. The maximum solar radiation was 1218.19 μmol photons m^{-2} s^{-1} at 11:58 am (Figure 2A). During the 2-weeks

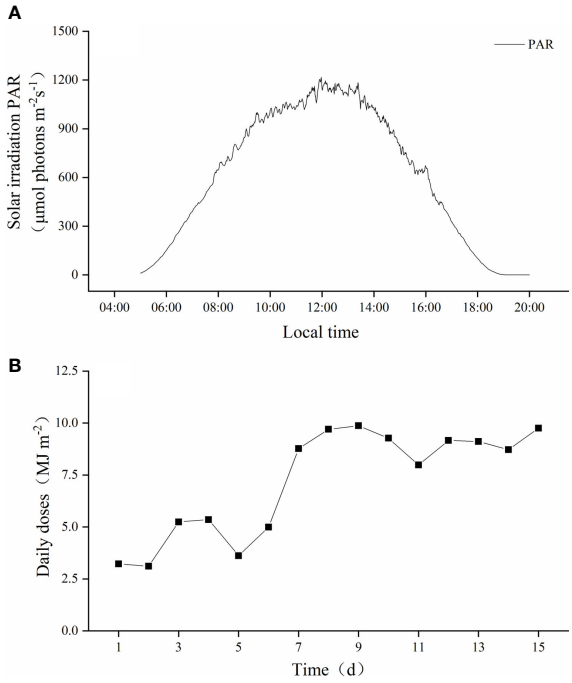

FIGURE 2
The average daily variation of the outdoor solar radiation **(A)** and daily cumulative variation **(B)** for 15 days during the experiment.

culture duration, the average daily dose was 7.19 MJ m^{-2}, and the maximum and minimum values were 9.76 MJ m^{-2} on the ninth day and 3.11 MJ m^{-2} on the second day, respectively (Figure 2B).

3.2 Carbonate system

The seawater carbonate systems of all treatments were recorded (Table 1). pCO_2 and nutrient conditions had a significant interactive effect on seawater pH and CO_3^{2-} ($P< 0.05$). The pH under HC conditions were lower by about 0.3 units compared to that under LC conditions. Moreover, DIC, HCO_3^-, CO_3^{2-} and CO_2 were higher by 8.4%, higher by 11.7%, lower by 42.9%, and higher by 119% compared to those under LC conditions, respectively.

3.3 Growth

As shown in Figure 3, there was a significant interaction between pCO_2 and nutrient conditions on the relative growth rate (RGR) of *U. prolifera* ($P< 0.05$). The RGR of *U. prolifera* in each treatment group were 52.95% d^{-1} under HCHN, 55.91% d^{-1} under LCHN, 32.87% d^{-1} under HCNN and 29.68% d^{-1} under LCNN. Compared with NN, HN significantly improved the *U. prolifera* growth both under HC and LC conditions ($P< 0.05$). Meanwhile, the thalli RGR increased by 61.10% under HCHN and 88.39% under LCHN compared to those under HCNN and LCNN, respectively. Under HN, HC significantly decreased the *U. prolifera* RGR ($P< 0.05$), which was lower by 5.30% compared to that in LC condition.

TABLE 1 Seawater carbonate system parameters under different culture conditions.

Treatments	pCO_2 (μatm)	pH	TA (μmol Kg^{-1})	DIC (μmol Kg^{-1})	HCO_3^- (μmol Kg^{-1})	CO_3^{2-} (μmol Kg^{-1})	CO_2 (μmol Kg^{-1})
HCHN	1013.93 ± 39.67^{A*}	7.84 ± 0.02^{A*}	2305.60 ± 22.59^{A}	2208.21 ± 19.44^{A*}	2089.96 ± 17.86^{A*}	84.60 ± 3.57^{A*}	33.64 ± 1.32^{A*}
HCNN	988.37 ± 26.43^{A*}	7.85 ± 0.01^{A*}	2324.33 ± 38.47^{A}	2221.98 ± 38.49^{A*}	2101.52 ± 36.75^{A*}	87.67 ± 1.37^{A*}	32.79 ± 0.88^{A*}
LCHN	451.67 ± 22.96^{a}	8.14 ± 0.02^{a}	2254.40 ± 85.86^{a}	2039.50 ± 79.10^{a}	1872.16 ± 72.10^{a}	152.36 ± 8.35^{a}	14.99 ± 0.76^{a}
LCNN	464.35 ± 3.10^{a}	8.13 ± 0.01^{a}	2256.92 ± 20.12^{a}	2046.53 ± 16.28^{a}	1881.54 ± 13.36^{a}	149.58 ± 3.04^{a}	15.41 ± 0.10^{a}

Different capital letters indicate significant differences between HN and NN under HC, and different lowercase letters indicate significant differences between HN and NN under LC. HC=1000 μatm; LC=air; HN=135 μmol L^{-1} N, 8.5 μmol L^{-1} P; NN=27 μmol L^{-1} N, 1.7 μmol L^{-1} P. Symbols (*) represent significant differences between LC and HC under the same nutrient conditions. Data are presented as means ± standard deviation (n = 3).

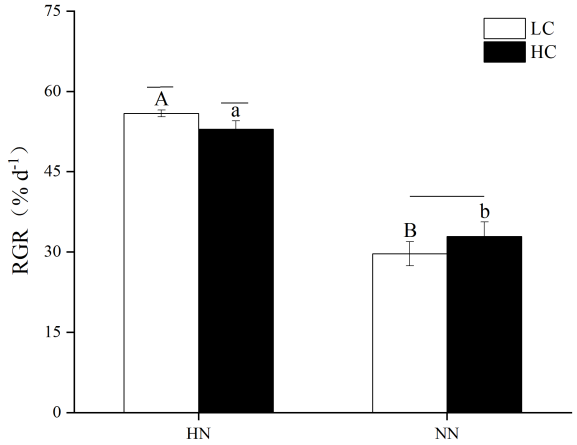

FIGURE 3
Relative growth rate (RGR) of *Ulva prolifera* during the first 8 days of the experiment. HC=1000 µatm; LC=air; HN=135 µmol L^{-1} N, 8.5 µmol L^{-1} P; NN=27 µmol L^{-1} N, 1.7 µmol L^{-1} P. Error bars represent standard deviation (n=3). Different capital letters indicate significant differences between HN and NN treatments under HC condition, and different lowercase letters indicate significant differences between HN and NN treatments under LC condition. The horizontal straight line indicates whether there is a significant difference between the HC and LC treatments within a nutrient concentration treatment.

3.4 Chlorophyll fluorescence parameters

As shown in Figure 4, the fluorescence yield (Yield) of HCNN was 0.48 ± 0.01 at 8:00, which was significantly higher than those in the other treatments at the same time ($P< 0.05$). Yield of HCNN, LCHN and LCNN reached the lowest value at 14:00. Yield of HCHN had two minimum values of 0.21 ± 0.02 at 10:00 and 0.21 ± 0.01 at 12:00 and reached the maximum value of 0.34 ± 0.01 at 14:00, which was significantly higher than those in the other treatments at the same time ($P< 0.05$).

The photosynthetic properties of *U. prolifera* under different culture conditions were shown in Figure 5 and Table 2. pCO_2 and nutrient concentrations had a very significant interactive effect on chlorophyll fluorescence parameters α and $rETR_{max}$ ($P< 0.01$), and there was a significant interaction on I_k ($P< 0.05$). Compared with LCNN, α significantly decreased by 39.13% under LCHN ($P< 0.05$). The $rETR_{max}$ of *U. prolifera* decreased by 14.51% under HCHN and decreased by 21.43% under LCHN compared to those under HCNN and LCNN, respectively. Nutrient concentrations had no significant effect on I_k under HC or LC ($P > 0.05$).

3.5 Photosynthetic rate

Net photosynthetic rate (P_m) of *U. prolifera* under different culture conditions was shown in Figure 6 and Table 3. There was no significant interaction between pCO_2 and nutrient concentrations ($P > 0.05$). Under LC or HC, the maximum P_m of HN condition was higher than that of NN condition. Compared with HCHN, the P_m of HCNN was significantly increased by 48.69% ($P< 0.05$). HCHN

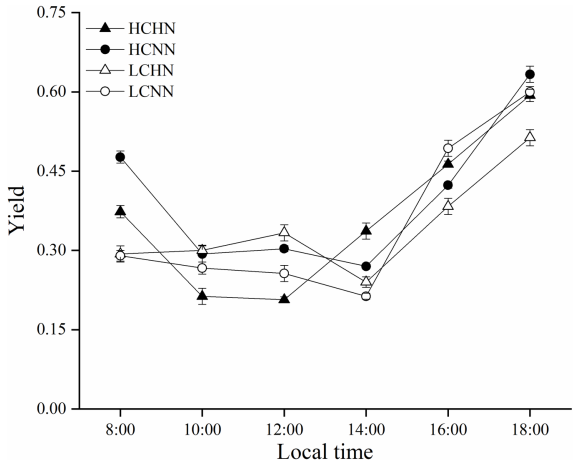

FIGURE 4
Diurnal variation of fluorescence yield (Yield) of HN and NN treatments in *Ulva prolifera* under different CO_2 concentrations. HC=1000 µatm; LC=air; HN=135 µmol L^{-1} N, 8.5 µmol L^{-1} P; NN=27 µmol L^{-1} N, 1.7 µmol L^{-1} P. Error bars represent standard deviation (n=3).

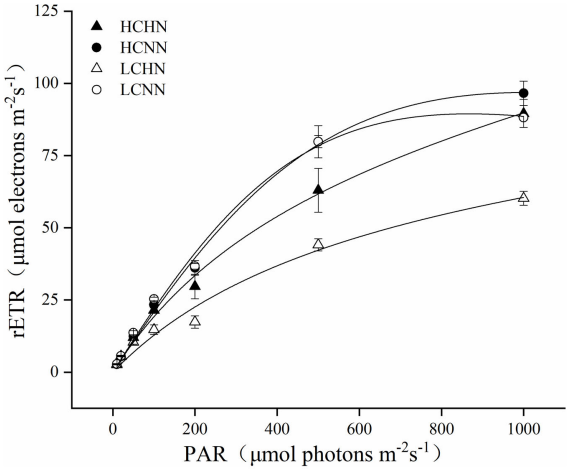

FIGURE 5
Relative electron transfer rate (rETR) for HN and NN treatments in *Ulva prolifera* under different CO_2 concentrations. HC=1000 μatm; LC=air; HN=135 μmol L^{-1} N, 8.5 μmol L^{-1} P; NN=27 μmol L^{-1} N, 1.7 μmol L^{-1} P. Error bars represent standard deviation (n=3).

significantly increased light energy utilization rate (α) of *U. prolifera* ($P< 0.05$), the value of which higher by 25.71% compared to that under HCNN. The R_d and I_c of HCHN were significantly increased by 57.47% and reduced by 49.12% compared to those under HCNN ($P< 0.05$), respectively. Moreover, the I_c of *U. prolifera* under LCHN decreased by 39.86% compared to that under LCNN.

3.6 Photosynthetic pigments

The contents of photosynthetic pigments in *U. prolifera* under different treatments were shown in Figure 7, pCO_2 and nutrient concentrations had a highly significant interaction on the contents of chlorophyll *a* and carotenoids ($P< 0.01$). There was a significant interaction on the chlorophyll *b* content ($P< 0.05$). The chlorophyll *a* contents were higher by 77.17% under LCHN and 37.02% under HCHN compared to those under LCNN and HCNN ($P< 0.05$), respectively. Under NN, HC significantly increased the chlorophyll *a* content, which was higher by 17.81% compared to that under LC ($P< 0.05$).

pCO_2 and nutrient concentrations had a significant interaction on the chlorophyll *b* content ($P< 0.05$). The chlorophyll *b* content under LCHN increased by 108.40% compared to that under LCNN ($P< 0.05$). Under NN, HC significantly increased the content of chlorophyll *b* ($P< 0.05$), which was higher by 31.07% compared to that in LC condition.

The effects of pCO_2 and nutrient concentrations on the carotenoid content were different from those on the above two photosynthetic pigments. Under HC, HN significantly decreased the carotenoid content compared with that under NN ($P< 0.05$). Under LC, the carotenoid content in HN condition significantly increased by 20.23% compared to that in NN condition ($P< 0.05$). Under HN, HC significantly decreased the carotenoid content ($P< 0.05$), which was lower by 65.80% compared to that in LC condition.

3.7 Soluble carbohydrates

The variability of soluble carbohydrate contents in different culture conditions was shown in Figure 8A. There was a significant interaction between pCO_2 and nutrient concentrations ($P< 0.05$). The soluble carbohydrate content in HCHN condition was significantly decreased by 46.94% compared to that in HCNN condition ($P< 0.05$). Under LC, the soluble carbohydrate content in HN condition was significantly reduced by 43.96% compared to that in NN condition ($P< 0.05$). The soluble carbohydrate content under HCNN was significantly increased by 26.73% compared to that under LCNN ($P< 0.05$).

TABLE 2 Rapid light response curve chlorophyll fluorescence parameters of *Ulva prolifera* under different culture conditions.

Treatments	α	$rETR_{max}$	I_k
HCHN	$0.22 \pm 0.02^{A*}$	$83.27 \pm 1.46^{B*}$	381.65 ± 37.27^{A}
HCNN	0.22 ± 0.02^{A}	97.40 ± 4.66^{A}	457.04 ± 70.10^{A}
LCHN	0.14 ± 0.03^{b}	73.75 ± 0.17^{b}	528.91 ± 125.87^{a}
LCNN	0.23 ± 0.02^{a}	89.56 ± 1.05^{a}	396.12 ± 34.36^{a}

Different capital letters indicate significant differences between HN and NN under HC, and different lowercase letters indicate significant differences between HN and NN under LC. HC=1000 μatm; LC=air; HN=135 μmol L^{-1} N, 8.5 μmol L^{-1} P; NN=27 μmol L^{-1} N, 1.7 μmol L^{-1} P. Symbols (*) represent significant differences between LC and HC under the same nutrient conditions. Data are means ± standard deviation (n = 3).

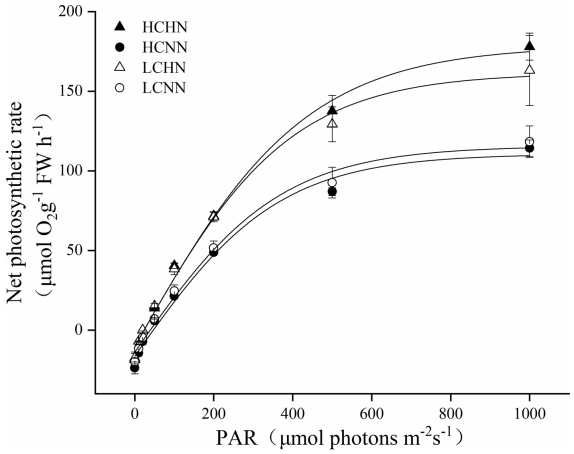

FIGURE 6
Net photosynthetic rate of HN and NN treatments in *Ulva prolifera* under different CO_2 concentrations. HC=1000 μatm; LC=air; HN=135 μmol L^{-1} N, 8.5 μmol L^{-1} P; NN=27 μmol L^{-1} N, 1.7 μmol L^{-1} P. Error bars represent standard deviation (n=3).

3.8 Soluble protein

The contents of soluble protein in *U. prolifera* under different culture conditions were relatively stable, ranging from 39.84 ± 0.07 mg g^{-1} FW to 41.16 ± 0.06 mg g^{-1} FW. pCO_2 and nutrient concentrations had a significant interaction ($P< 0.05$). As shown in Figure 8B, Under HC, HN significantly increased soluble protein content ($P< 0.05$), which was higher by 2.95% compared to that under NN. The soluble protein content under HCNN decreased by 2.59% compared to that under LCNN.

3.9 Nitrate reductase activity

There was no significant interaction between pCO_2 and nutrient concentrations on the nitrate reductase activity of *U. prolifera* ($P > 0.05$). As shown in Figure 9, the nitrate reductase activity of *U. prolifera* under HN was higher than that under NN. HCHN significantly increased the nitrate reductase activity ($P< 0.05$), which was higher by 129.08% compare to that under HCNN. Moreover, LCHN significantly increased the nitrate reductase activity, which was higher by 159.89% compared with that under LCNN ($P< 0.05$).

4 Discussion

In eutrophic estuaries and nearshore regions, opportunistic green algae have a high biomass, accounting for 68%, especially *Ulva* spp., accompanied by a high drift rate (Potter et al., 2021). The algae density affects the stability of seawater carbonate systems. To maintain a stable carbonate system in the seawater, algae biomass should be kept within a range of 2.0 ± 0.1 g L^{-1} (Liu et al., 2012). In order to obtain a more ideal carbonate stabilization system, the biomass of *Ulva* spp. in many studies was consistently controlled below 0.4 g L^{-1} (Gao et al., 2012; Gao et al., 2016; Gao et al., 2017a; Gao et al., 2018; Gao et al., 2019b). In this study, initial biomass of *U. prolifera* was 0.1 g L^{-1} and the final harvested biomass was less than 0.4 g L^{-1}, which could meet the stability requirements of the seawater carbonate system. The results of this study showed that the relative growth rates of *U. prolifera* under HN conditions were significantly increased under HC or LC condition, and the amounts of Chl *a* and Chl *b* under HN treatment were significantly higher than those under NN treatment. Under HN treatment, the maximum net photosynthetic rate and light energy utilization of *U. prolifera* were higher than those under NN treatment. The increment of photosynthetic pigment content can promote light energy absorption rate by algae and thus enhance the photosynthetic rate (Zhou et al., 2022). In this experiment, a significant improvement of the maximum photosynthetic

TABLE 3 Net photosynthetic rate parameters of *Ulva prolifera* under different culture conditions.

Treatments	P_m	α	R_d	I_k	I_c
HCHN	188.79 ± 10.18^{A}	0.44 ± 0.02^{A}	-10.37 ± 1.09^{A}	432.50 ± 13.28^{A}	23.75 ± 2.15^{B}
HCNN	126.97 ± 4.48^{B}	0.35 ± 0.02^{B}	-16.33 ± 1.42^{B}	364.43 ± 32.22^{A}	46.68 ± 1.79^{A}
LCHN	172.08 ± 24.42^{a}	0.44 ± 0.01^{a}	-10.24 ± 1.02^{a}	392.66 ± 49.86^{a}	23.39 ± 2.13^{b}
LCNN	129.35 ± 12.63^{b}	0.35 ± 0.05^{a}	-13.81 ± 3.24^{a}	368.76 ± 19.15^{a}	38.89 ± 5.07^{a}

Different capital letters indicate significant differences between HN and NN under HC, and different lowercase letters indicate significant differences between HN and NN under LC. HC=1000 μatm; LC=air; HN=135 μmol L^{-1} N, 8.5 μmol L^{-1} P; NN=27 μmol L^{-1} N, 1.7 μmol L^{-1} P. Data are means ± standard deviation (n = 3).

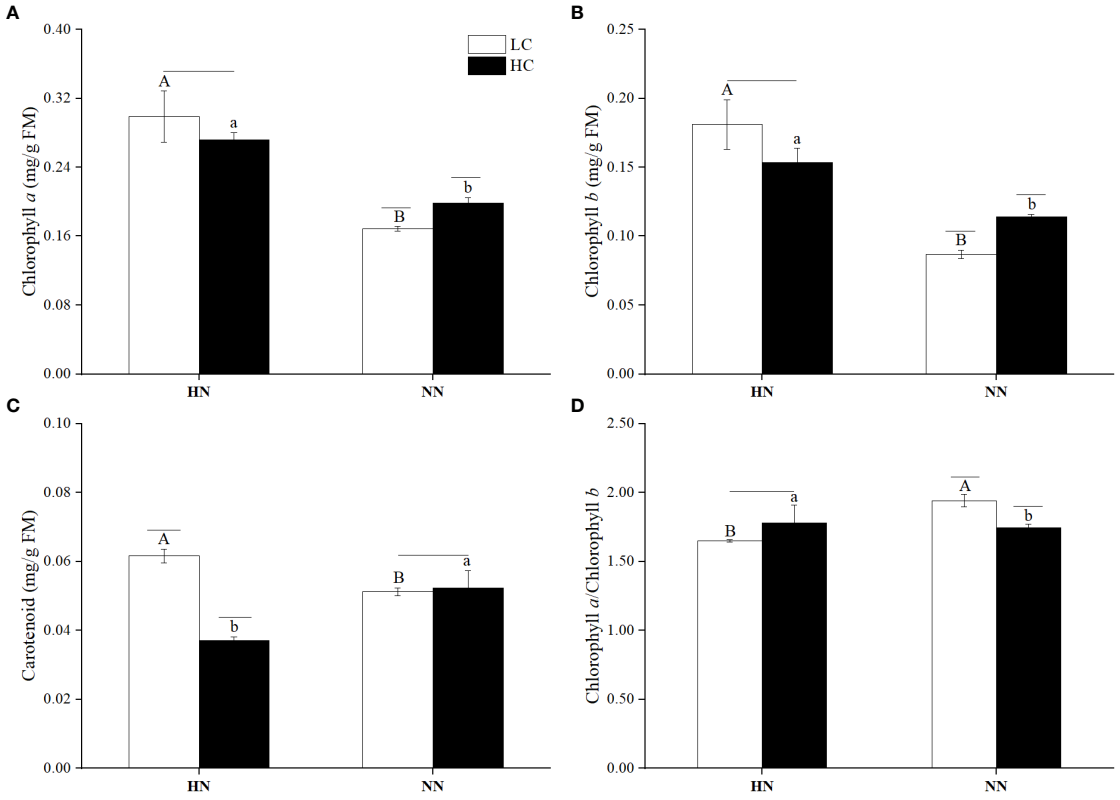

FIGURE 7
The contents of Chlorophyll *a* **(A)**, Chlorophyll *b* **(B)**, Carotenoid **(C)** and the ratio of chlorophyll *a* to chlorophyll *b* **(D)** in *Ulva prolifera* under different culture conditions. HC=1000 µatm; LC=air; HN=135 µmol L^{-1} N, 8.5 µmol L^{-1} P; NN=27 µmol L^{-1} N, 1.7 µmol L^{-1}P. Error bars represent standard deviation (n=3). Different capital letters indicate significant differences between HN and NN treatments under HC condition, and different lowercase letters indicate significant differences between HN and NN treatments under LC condition. The horizontal straight line indicates whether there is a significant difference between the HC and LC treatments within a nutrient concentration treatment.

rate under HN treatment also confirmed that algae can adapt to environmental changes by adjusting the contents of photosynthetic pigments (Gao et al., 2018). It was proved that eutrophication treatments remarkably increased the photosynthesis rate of *U. prolifera* and further promoted algae growth. A similar phenomenon had also been reported in *U. rigida* (Gao et al., 2017a). This may be due to an increment in the phosphate absorption rate. In addition, the increased phosphorus concentration had a obvious promotion effect on the nitrate absorption rate, which was a favorable influence on macroalgae growth (Wang et al., 2019).

Interestingly, here elevated pCO_2 significantly inhibited the relative growth rate of *U. prolifera* under eutrophication conditions ($P< 0.05$). The results showed that the amount of carotenoid in *U. prolifera* was significantly decreased under HCHN conditions. The carotenoid content under LCHN was 65.80% higher than that under HCHN. Macroalgae cultivated outdoors was inevitably exposed to high light intensity and was affected by highlight stress. In this study, solar radiation at noon reached the maximum range throughout the day (Figure 2A), and Yield of *U. prolifera* under HCHN reached the minimum range, which were significantly lower than that under LCHN (Figure 4). It might be due to the photodamage caused by the downregulation of high light intensity or carbon dioxide concentration mechanism (CCMs) (Xu and Gao, 2010; Gao et al., 2016; Van Alstyne, 2018). Moreover, in light harvesting complex, carotenoids play a very important role in preventing photodamage caused by excess light intensity (Fu et al., 2013). However, the results showed that elevated pCO_2 was not conducive to carotenoid synthesis of *U. prolifera* under eutrophication conditions, which potentially enhanced the chance of thalli photodamage and further aggravated the inhibition of algae growth. It may also be one of the important reasons that elevated pCO_2 inhibited the growth rate of *U. prolifera*. A similar phenomenon has been found in many marine macroalgae, such as the intertidal red macroalgae *Gracilaria tenuistipitata* (Vega et al., 2020), *G. lemaneiformis* (Qu et al., 2017) and *Neopyropia yezoensis* (Sun et al., 2021), the intertidal green macroalga *Bryopsis corticulans* (Giovagnetti et al., 2018) and the brown macroalgae *Lessonia spicata* (Zúñiga et al., 2020) and *Cystoseira tamariscifolia* (Celis-Plá et al., 2017). The amounts of Chl *a* and Chl *b* in *U. prolifera* increased significantly with increasing CO_2 under NN condition ($P< 0.05$), but the relative growth rate did not change significantly, which may be due to photoinhibition caused by high light intensity.

In addition to the physiological parameters of photosynthesis, the amounts of SC and SP in *U. prolifera* were varied under different conditions. The results of this experiment showed that the SC under

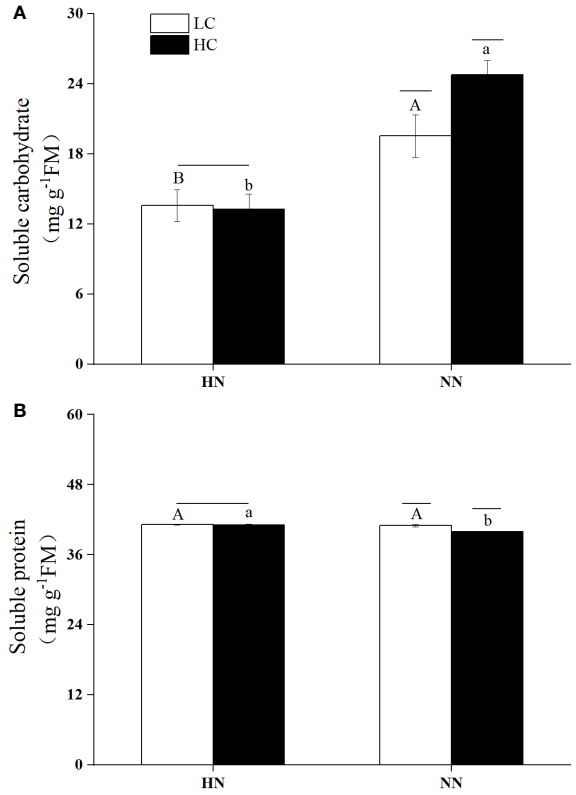

FIGURE 8
The contents of soluble carbohydrate **(A)** and soluble protein **(B)** of *Ulva prolifera* under different culture conditions. HC=1000 µatm; LC=air; HN=135 µmol L^{-1} N, 8.5 µmol L^{-1} P; NN=27 µmol L^{-1} N, 1.7 µmol L^{-1} P; Error bars represent standard deviation (n=3). Different capital letters indicate significant differences between HN and NN treatments under HC conditions, and different lowercase letters indicate significant differences between HN and NN treatments under LC condition. The horizontal straight line indicates whether there is a significant difference between the HC and LC treatments within a nutrient concentration treatment.

HN was significantly lower than that under NN, which may be related to the higher relative growth rate under HN than that under NN. Under NN, the soluble carbohydrate content of *U. prolifera* in HC condition was significantly increased compared with that in LC condition. This may be related to the higher Yield and rETR under HCNN condition. It is different from *U. compressa*, the total SC level of which significantly decreased by about 19% under acidification (Vinuganesh et al., 2022). The reason may be that

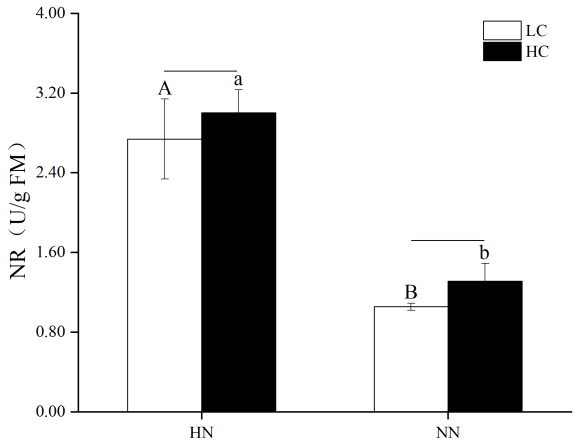

FIGURE 9
Nitrate reductase activity (NR) of *Ulva prolifera* under different culture conditions. HC=1000 µatm; LC=air; HN=135 µmol L^{-1}N, 8.5 µmol L^{-1} P; NN=27 µmol L^{-1} N, 1.7 µmol L^{-1} P. Error bars represent standard deviation (n=3). Different capital letters indicate significant differences between HN and NN treatments under HC condition, and different lowercase letters indicate significant differences between HN and NN treatments under LC condition. The horizontal straight line indicates whether there is a significant difference between the HC and LC treatments within a nutrient concentration treatment.

other substances involved in soluble carbohydrates are altered in response to acidification (Sun et al., 2021). In this study, HNHC significantly increased the SP amount of *U. prolifera* compared with NNHC treatment. This is consistent with the result that HN significantly increased the nitrate reductase activity of *U. prolifera* compared with NN under HC conditon. It can be attributed to the increase of protein synthesis caused by the stimulation of NR under HC (Gordillo et al., 2001). The higher NR also matched the higher RGR under HN condition in *U. prolifera*. In green algae, high nitrate conditions were beneficial to the synthesis of proteins and lipids (El-Sayed et al., 2022). It may lead to more severe green tides when near-shore eutrophication is not effectively managed (Gao et al., 2017b).

5 Conclusion

Due to the excessive use of fossil fuels, the atmospheric CO_2 concentration is increasing year by year, and ocean acidification is becoming increasingly serious. At the same time, the excessive discharge of nutrients in the coastal waters leads to large areas of eutrophication in nearshore waters. Eutrophication was the main factor, which significantly increased the relative growth rate and photosynthesis of *U. prolifera*. Acidification did not play a driving role in promoting *U. prolifera* growth, and even inhibited its growth under eutrophication conditions, especially on sunny days. This suggests that seawater eutrophication would greatly accelerate *U. prolifera* bloom, which may also be suppressed to a certain extent by ocean acidification in the future. The study can provide valuable information for predicting the future outbreaks of *U. prolifera* green tide in nearshore regions.

Data availability statement

The original contributions presented in the study are included in the article/supplementary material. Further inquiries can be directed to the corresponding authors.

Author contributions

JX conceived and designed the experiments. JC, JN, WZ, ZC, SW, YL, and RW contributed to carry out the experiments. JC, WZ, CH, JW, and YL analyzed data. JC and WZ wrote the paper. JX, WZ, and JC revised the manuscript. All authors contributed to the article and approved the submitted version.

Funding

This work was supported by the special fund for Natural Resources Development (Innovation Project of Marine Science and Technology) of Jiangsu Province (JSZRHYKJ202107; JSZRHYKJ202206; JSZRHYKJ202001), the Modern Fisheries Industrial Research System of Jiangsu Province (JATS[2022]522), the College Student Innovation and Entrepreneurship Training Program of Jiangsu Province Higher Education (2019120284), the Talent Introduction Fund Project of Jiangsu Ocean University (KQ19068), the Huaguoshan Talent Project of Lianyungang, and Priority Academic Program Development of Jiangsu Higher Education Institutions.

Conflict of interest

The authors declare that the research was conducted in the absence of any commercial or financial relationships that could be construed as a potential conflict of interest.

Publisher's note

References

Barakat, K. M., El-Sayed, H. S., Khairy, H. M., El-Sheikh, M. A., Al-Rashed, S. A., Arif, I. A., et al. (2021). Effects of ocean acidification on the growth and biochemical composition of a green alga (*Ulva fasciata*) and its associated microbiota. *Saudi. J. Biol. Sci.* 28 (9), 5106–5114. doi: 10.1016/j.sjbs.2021.05.029

Bradford, M. M. (1976). A rapid and sensitive method for the quantitation of microgram quantities of protein utilizing the principle of protein-dye binding. *Anal. Biochem.* 72, 248–254. doi: 10.1016/0003-2697(76)90527-3

Celis-Plá, P. S., Martínez, B., Korbee, N., Hall-Spencer, J. M., and Figueroa, F. L. (2017). Ecophysiological responses to elevated CO_2 and temperature in *Cystoseira tamariscifolia* (Phaeophyceae). *Clim. Change* 142, 67–81. doi: 10.1007/s10584-017-1943-y

Cruces, E., Rautenberger, R., Cubillos, V. M., Ramírez-Kushel, E., Rojas-Lillo, Y., Lara, C., et al. (2019). Interaction of photoprotective and acclimation mechanisms in *Ulva rigida* (Chlorophyta) in response to diurnal changes in solar radiation in southern Chile. *J. Appl. Phycol.* 55 (5), 1011–1027. doi: 10.1111/jpy.12894

Cui, J., Monotilla, A. P., Zhu, W., Takano, Y., Shimada, S., Ichihara, K., et al. (2018). Taxonomic reassessment of *U. prolifera* (Ulvophyceae, chlorophyta) based on specimens from the type locality and yellow Sea green tides. *Phycologia* 57 (6), 692–704. doi: 10.2216/17-139.1

Deriaz, R. E. (1961). Routine analysis of carbohydrates and lignin in herbage. *J. Sci. Food Agric.* 12, 152–160. doi: 10.1002/jsfa.2740120210

Doney, S. C., Fabry, V. J., Feely, R. A., and Kleypas, J. A. (2009). Ocean acidification: the other CO_2 problem. *Ann. Rev. Mar. Sci.* 1, 169–192. doi: 10.1146/annurev.marine.010908.163834

El-Sayed, H. S., Elshobary, M. E., Barakat, K. M., Khairy, H. M., El-Sheikh, M. A., Czaja, R., et al. (2022). Ocean acidification induced changes in *Ulva fasciata* biochemistry may improve dicentrarchus labrax aquaculture *via* enhanced antimicrobial activity. *Aquaculture* 560 (15), 738474. doi: 10.1016/j.aquaculture.2022.738474

Feely, R. A., Doney, S. C., and Cooley, S. R. (2009). Ocean acidification: Present conditions and future changes in a high-CO_2 world. *Oceanography* 22 (4), 36–47. doi: 10.5670/oceanog.2009.95

Franz, D. R., and Friedman, I. (2002). Effects of a macroalgal mat (*Ulva lactuca*) on estuarine sand flat copepods: an experimental study. *J. Exp. Mar. Biol. Ecol.* 271 (2), 209–226. doi: 10.1016/S0022-0981(02)00045-X

Fu, W., Guðmundsson, Ó., Paglia, G., Herjólfsson, G., Andrésson, Ó. S., Palsson, B. Ø., et al. (2013). Enhancement of carotenoid biosynthesis in the green microalga *Dunaliella salina* with light-emitting diodes and adaptive laboratory evolution. *Appl. Microbiol. Biotechnol.* 97, 2395–2403. doi: 10.1007/s00253-012-4502-5

Gao, G., Beardall, J., Bao, M., Wang, C., Ren, W., and Xu, J. (2018). Ocean acidification and nutrient limitation synergistically reduce growth and photosynthetic performances of a green tide alga *Ulva linza*. *Biogeosciences* 15 (11), 3409–3420. doi: 10.5194/bg-15-3409-2018

Gao, G., Clare, A. S., Rose, C., and Caldwell, G. S. (2017a). Eutrophication and warming-driven green tides (*Ulva rigida*) are predicted to increase under future climate change scenarios. *Mar. pollut. Bull.* 114 (1), 439–447. doi: 10.1016/j.marpolbul.2016.10.003

Gao, G., Clare, A. S., Rose, C., and Caldwell, G. S. (2017b). Intrinsic and extrinsic control of reproduction in the green tide-forming alga, *Ulva rigida*. *Environ. Exp. Bot.* 139, 14–22. doi: 10.1016/j.envexpbot.2017.03.016

Gao, G., Fu, Q., Beardall, J., Wu, M., and Xu, J. (2019a). Combination of ocean acidification and warming enhances the competitive advantage of *Skeletonema costatum* over a green tide alga, *Ulva linza*. *Harmful. Algae.* 85, 101698. doi: 10.1016/j.hal.2019.101698

Gao, G., Liu, Y., Li, X., Feng, Z., and Xu, J. (2016). An ocean acidification acclimatised green tide alga is robust to changes of seawater carbon chemistry but vulnerable to light stress. *PLoS. One* 11 (12), e0169040. doi: 10.1371/journal.pone.0169040

Gao, G., Qu, L., Xu, T., Burgess, J. G., Li, X., and Xu, J. (2019b). Future CO_2-induced ocean acidification enhances resilience of a green tide alga to low-salinity stress. *ICES. J. Mar. Sci.* 76 (7), 2437–2445. doi: 10.1093/icesjms/fsz135

Gao, K., Xu, J., Gao, G., Li, Y., Hutchins, D. A., Huang, B., et al. (2012). Rising CO_2 and increased light exposure synergistically reduce marine primary productivity. *Nature. Clim. Change.* 2 (7), 519–523. doi: 10.1038/NCLIMATE1507

Gattuso, J. P., Magnan, A., Billé, R., Cheung, W. W., Howes, E. L., Joos, F., et al. (2015). Contrasting futures for ocean and society from different anthropogenic CO_2 emissions scenarios. *Science* 349 (6243), aac4722. doi: 10.1126/science.aac4722

Genty, B., Briantais, J. M., and Baker, N. R. (1989). The relationship between the quantum yield of photosynthetic electron transport and quenching of chlorophyll fluorescence. *Biochim. Biophys. Acta (BBA)-General. Subj.* 990 (1), 87–92. doi: 10.1016/S0304-4165(89)80016-9

Giovagnetti, V., Han, G., Ware, M. A., Ungerer, P., Qin, X., Wang, W. D., et al. (2018). A siphonous morphology affects light-harvesting modulation in the intertidal green macroalga *Bryopsis corticulans* (Ulvophyceae). *Planta* 247, 1293–1306. doi: 10.1007/s00425-018-2854-5

Gordillo, F. J., Niell, F. X., and Figueroa, F. L. (2001). Non-photosynthetic enhancement of growth by high CO_2 level in the nitrophilic seaweed *Ulva rigida* c. agardh (Chlorophyta). *Planta* 213 (1), 64–70. doi: 10.1007/s004250000468

Henley, W. J. (1993). Measurement and interpretation of photosynthetic light-response curves in algae in the context of photoinhibition and diel changes. *J. Phycol.* 29, 729–739. doi: 10.1111/j.0022-3646.1993.00729.x

Hoegh-Guldberg, O., Mumby, P. J., Hooten, A. J., Steneck, R. S., Greenfield, P., Gomez, E., et al. (2007). Coral reefs under rapid climate change and ocean acidification. *Science* 318 (5857), 1737–1742. doi: 10.1126/science.1152509

Huo, Y., Kim, J. K., Yarish, C., Augyte, S., and He, P. (2021). Responses of the germination and growth of *U. prolifera* parthenogametes, the causative species of green tides, to gradients of temperature and light. *Aquat. Bot.* 170, 103343. doi: 10.1016/j.aquabot.2020.103343

Kang, E. J., Han, A. R., Kim, J. H., Kim, I. N., Lee, S., Min, J. O., et al. (2021). Evaluating bloom potential of the green-tide forming alga *Ulva ohnoi* under ocean acidification and warming. *Sci. Total. Environ.* 769, 144443. doi: 10.1016/j.scitotenv.2020.144443

Kühl, M., Chen, M., Ralph, P. J., Schreiber, U., and Larkum, A. W. (2005). A niche for cyanobacteria containing chlorophyll *d*. *Nature* 433 (7028), 820–820. doi: 10.1038/433820a

Lewis, E., Wallace, D., and Allison, L. J. (1998). *Program developed for CO2 system calculations (No. ORNL/CDIAC-105)* (Upton, NY (United States: Brookhaven National Lab., Dept. of Applied Science). Oak Ridge National Lab., Carbon Dioxide Information Analysis Center, TN (United States).

Liu, F., Pang, S., Chopin, T., Gao, S., Shan, T., Zhao, X., et al. (2013). Understanding the recurrent large-scale green tide in the yellow Sea: Temporal and spatial correlations between multiple geographical, aquacultural and biological factors. *Mar. Environ. Res.* 83, 38–47. doi: 10.1016/j.marenvres.2012.10.007

Liu, Y., Xu, J., and Gao, K. (2012). CO_2-driven seawater acidification increases photochemical stress in a green alga. *Phycologia* 51 (5), 562–566. doi: 10.2216/11-65.1

Olischläger, M., Bartsch, I., Gutow, L., and Wiencke, C. (2013). Effects of ocean acidification on growth and physiology of *Ulva lactuca* (Chlorophyta) in a rockpool-scenario. *Phycological. Res.* 61 (3), 180–190. doi: 10.1111/pre.12006

Potter, I. C., Rose, T. H., Huisman, J. M., Hall, N. G., Denham, A., and Tweedley, J. R. (2021). Large Variations in eutrophication among estuaries reflect massive differences in composition and biomass of macroalgal drift. *Mar. pollut. Bull.* 167, 112330. doi: 10.1016/j.marpolbul.2021.112330

Qu, L., Xu, J., Sun, J., Li, X., and Gao, K. (2017). Diurnal pH fluctuations of seawater influence the responses of an economic red macroalga *Gracilaria lemaneiformis* to future CO_2-induced seawater acidification. *Aquaculture* 473, 383–388. doi: 10.1016/j.aquaculture.2017.03.001

Ralph, P. J., and Gademann, R. (2005). Rapid light curves: a powerful tool to assess photosynthetic activity. *Aquat. Bot.* 82 (3), 222–237. doi: 10.1016/j.aquabot.2005.02.006

Reidenbach, L. (2017). "The effects of ocean acidification and eutrophication on the macroalgae ulva spp," in *Doctoral dissertation* (Northridge: California State University).

Sun, J., Bao, M., Xu, T., Li, F., Wu, H., Li, X., et al. (2021). Elevated CO_2 influences competition for growth, photosynthetic performance and biochemical composition in *Neopyropia yezoensis* and *Ulva. prolifera*. *Algal. Res.* 56, 102313. doi: 10.1016/j.algal.2021.102313

Tan, I. H., Blomster, J., Hansen, G., Leskinen, E., Maggs, C. A., Mann, D. G., et al. (1999). Molecular phylogenetic evidence for a reversible morphogenetic switch controlling the gross morphology of two common genera of green seaweeds, *Ulva* and *Enteromorpha*. *Mol. Biol. Evol.* 16 (8), 1011–1018. doi: 10.1007/PL00008639

Van Alstyne, K. L. (2018). Seawater nitrogen concentration and light independently alter performance, growth, and resource allocation in the bloom-forming seaweeds *Ulva lactuca* and *Ulvaria obscura* (Chlorophyta). *Harmful. Algae.* 78, 27–35. doi: 10.1016/j.hal.2018.07.005

Vega, J., Bonomi-Barufi, J., Gómez-Pinchetti, J. L., and Figueroa, F. L. (2020). Cyanobacteria and red macroalgae as potential sources of antioxidants and UV radiation-absorbing compounds for cosmeceutical applications. *Mar. Drugs* 18 (12), 659. doi: 10.3390/md18120659

Vinuganesh, A., Kumar, A., Prakash, S., Alotaibi, M. O., Saleh, A. M., Mohammed, A. E., et al. (2022). Influence of seawater acidification on biochemical composition and oxidative status of green algae *Ulva compressa*. *Sci. Total. Environ.* 806, 150445. doi: 10.1016/j.scitotenv.2021.150445

Wang, C., Su, R., Guo, L., Yang, B., Zhang, Y., Zhang, L., et al. (2019). Nutrient absorption by *Ulva prolifera* and the growth mechanism leading to green-tides. *Estuar. Coast. Shelf. Sci.* 227, 106329. doi: 10.1016/j.ecss.2019.106329

Wang, Z., Xiao, J., Fan, S., Li, Y., Liu, X., and Liu, D. (2015). Who made the world's largest green tide in China ?–an integrated study on the initiation and early development of the green tide in yellow Sea. *Limnol* 60 (4), 1105–1117. doi: 10.1002/lno.10083

Wellburn, A. R. (1994). The spectral determination of chlorophylls *a* and *b*, as well as total carotenoids, using various solvents with spectrophotometers of different resolution. *J. Plant Physiol.* 144, 307–313. doi: 10.1016/S0176-1617(11)81192-2

Wu, Y. P., Gao, K. S., and Riebesell, U. (2010). CO_2-induced seawater acidification affects physiological performance of the marine diatom *Phaeodactylum tricornutum*. *Biogeosciences* 7, 2915–2923. doi: 10.5194/bg-7-2915-2010

Wu, H., Zhang, J., Yarish, C., He, P., and Kim, J. K. (2018). Bioremediation and nutrient migration during blooms of *Ulva* in the yellow Sea, China. *Phycologia* 57 (2), 223–231. doi: 10.2216/17-32.1

Xiao, Y., Zhang, J., Cui, T., Gong, J., Liu, R., Chen, X., et al. (2019). Remote sensing estimation of the biomass of floating *U. prolifera* and analysis of the main factors driving the interannual variability of the biomass in the yellow Sea. *Mar. pollut. Bull.* 140, 330–340. doi: 10.1016/j.marpolbul.2019.01.037

Xu, J., and Gao, K. (2010). UV-A enhanced growth and UV-b induced positive effects in the recovery of photochemical yield in *Gracilaria lemaneiformis* (Rhodophyta). *J. Photochem.* 100 (3), 117–122. doi: 10.1016/j.jphotobiol.2010.05.010

Xu, Z., Gao, G., Xu, J., and Wu, H. (2017). Physiological response of a golden tide alga (*Sargassum muticum*) to the interaction of ocean acidification and phosphorus enrichment. *Biogeosciences* 14 (3), 671–681. doi: 10.5194/bg-14-671-2017

Yabe, T., Ishii, Y., Amano, Y., Koga, T., Hayashi, S., Nohara, S., et al. (2009). Green tide formed by free-floating *Ulva* spp. at yatsu tidal flat, Japan. *Limnol* 10 (3), 239–245. doi: 10.1007/s10201-009-0278-4

Ye, N. H., Zhang, X. W., Mao, Y. Z., Liang, C. W., Xu, D., Zou, J., et al. (2011). 'Green tides' are overwhelming the coastline of our blue planet: taking the world's largest example. *Ecol. Res.* 26 (3), 477–485. doi: 10.1007/s11284-011-0821-8

Young, C. S., and Gobler, C. J. (2016). Ocean acidification accelerates the growth of two bloom-forming macroalgae. *PloS One* 11 (5), e0155152. doi: 10.1371/journal.pone.0155152

Yue, F., Gao, G., Ma, J., Wu, H., Li, X., and Xu, J. (2019). Future CO_2-induced seawater acidification mediates the physiological performance of a green alga *Ulva linza* in different photoperiods. *PeerJ* 7, e7048. doi: 10.7717/peerj.7048

Zhang, J., Huo, Y., Yu, K., Chen, Q., He, Q., Han, W., et al. (2013). Growth characteristics and reproductive capability of green tide algae in rudong coast, China. *J. Appl. Phycol.* 25 (3), 795–803. doi: 10.1007/s10811-012-9972-4

Zhou, W., Wu, H., Huang, J., Wang, J., Zhen, W., Wang, J., et al. (2022). Elevated-CO_2 and nutrient limitation synergistically reduce the growth and photosynthetic performances of a commercial macroalga *Gracilariopsis lemaneiformis*. *Aquaculture* 550, 737878. doi: 10.1016/j.aquaculture.2021.37878

Zúñiga, A., Sáez, C. A., Trabal, A., Figueroa, F. L., Pardo, D., Navarrete, C., et al. (2020). Seasonal photoacclimation and vulnerability patterns in the brown macroalga *Lessonia spicata* (Ochrophyta). *Water* 13 (1), 6. doi: 10.3390/w13010006